

Model Based Diagnosis of Leaks in the Air-Intake System of an SI-Engine

Mattias Nyberg, Andrej Perkovic

Vehicular Systems, ISY, Linköping University

S-581 83 Linköping, Sweden

e-mail: matny@isy.liu.se

phone: +46 13 282369

fax: +46 13 282035

ABSTRACT

One important area of SI-engine diagnosis is the diagnosis of leakage in the air-intake system. This is because a leakage can cause increased emissions and drivability problems. A method for accurately detecting leaks is presented. The results are developed for a turbo-charged engine but they are also valid for a naturally aspirated SI-engine. The method is based on a physical model of the leaks and includes an estimation of leakage area. By knowing the area, it is possible to reconfigure the control algorithm such that, the effect of the leak on emissions, is suppressed. As small leaks as 2 mm in diameter can be detected and it is possible to distinguish between leakages before or after the throttle. The method is suitable for on-line implementation.

1. INTRODUCTION

On-board diagnosis of car engines has become increasingly important because of environmentally based legislative regulations such as OBDII (On-Board Diagnostics) [1]. Other reasons for incorporating diagnosis in vehicles are repairability, availability and vehicle protection. Today, up to 50% of the engine management systems are dedicated to diagnosis.

One important area of SI (Spark Ignition) engine diagnosis is the diagnosis of leakage in the air-intake system. If the engine is equipped with an air-mass flow sensor, a leakage will result in that this sensor do not correctly measure the amount of air entering the combustion. This in turn will result in a deviation in the air-fuel ratio. A deviation in the air-fuel ratio is serious because it causes the emissions to increase when lambda do not equal 1 anymore, and also misfires can occur because of a too lean or rich mixture. In addition drivability will suffer and especially in turbo-charged engines, a leakage will result in loss of horsepowers.

Therefore the goal of this work is to find a method that can accurately detect leakages. It is important to detect leakages with an area as small as some square

millimeters. For the engine management, it is also important to get an estimate of the size of the leakage. This is to know what appropriate action that should be taken, e.g. give a warning to the driver. Additionally if the size of the leak is known, it is possible to reconfigure the control algorithm so that at least the increase in emissions, caused by the leak, will be small.

All experiments are performed on a turbo-charged engine and the method developed is able to detect and distinguish between leaks before and after the throttle. With this method it is possible to detect leaks as small as a hole with 2 mm in diameter, i.e. an area of 3.1 mm². The key technology is that the leaks are physically modeled as a flow through a restriction and then the diagnosis becomes a parameter identification problem.

The paper is organized as follows. In Section 2, the experimental setup is described. Section 3 and 4 describes the modeling of the air-intake system and the leaks. In Section 5, the principles of the estimation of leak area are provided. Finally Section 6 deals with on-line implementation issues and Section 7 contains the conclusion.

2. EXPERIMENTAL SETUP

All experiments were performed on a 4 cylinder, 2.3 liter, turbo-charged, spark-ignited SAAB production engine. It is constructed for the SAAB 9-5 model. The engine is mounted in a test bench together with a Schenck "DYNAS NT 85" AC dynamometer. Both during the model building and the validation, the engine were run according to Phase I+II of the FTP-75 test-cycle. The data for the test cycle had first been collected on a car with automatic transmission. This resulted in the engine speed and manifold pressure shown in Figure 1. In addition, static tests were performed in 172 different operating points defined by engine speed and manifold pressure.

Leaks were applied by using exchangeable bolts. One bolt were mounted in the wall of the manifold and the other in the wall of the air tube in front of the throt-

tle. The exchangeable bolts had drilled holes of different diameters ranging from 1 mm to 8 mm.

Data were collected by a DAQ-card mounted in a standard PC. All data were filtered with a LP-filter with a cutoff frequency of 2 Hz.

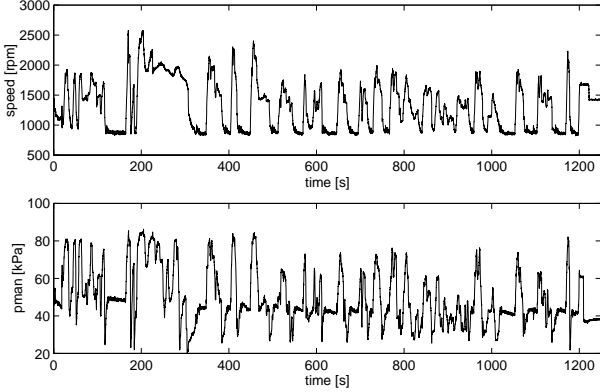


Fig. 1. Engine speed and manifold pressure during the FTP-75 test-cycle for a car with automatic transmission.

3. AIR-INTAKE SYSTEM MODEL

A schematic picture of the air-intake system is shown in Figure 2. Ambient air enters the system and an air-mass flow sensor measures the air-mass flow rate \dot{m}_s . Next, the air passes the compressor side of the turbo-charger and then the intercooler. This results in a *boost* pressure p_{boost} and temperature T that is higher than ambient pressure and temperature respectively. Next, the air passes the throttle and the flow \dot{m}_{th} is dependant on p_{boost} , T , the throttle angle α , and the manifold pressure p_{man} . Finally the air leaves the manifold and enters the cylinder. This flow \dot{m}_{cyl} is dependant on p_{man} and the engine speed n . Also shown in the figure are the two possible leaks: the *boost leak* somewhere between the air-mass flow sensor and the throttle, and the *manifold leak* somewhere in the manifold.

In this work, the air-intake system is modeled by a mean value model [2]. This means that no within cycle variations are covered by the model. A model is developed for the case when no leakage is present. Because there is no need for extremely fast detection of leakage, it is for the model, sufficient to consider only static relations. The model consists of two parts, the air-mass flow past the throttle and the air-mass flow into the cylinder.

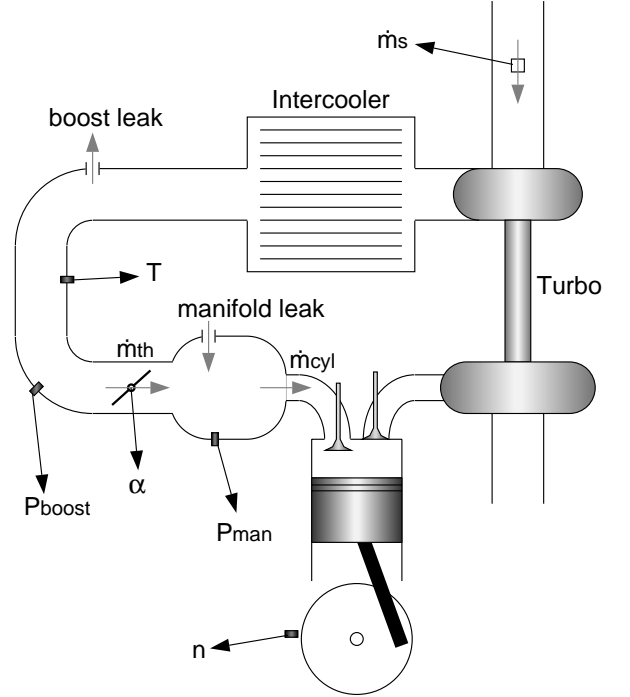


Fig. 2. The turbo-charged engine. Air-mass flows that are discussed in the text are marked with gray arrows.

3.1. Model of Air Flow Past Throttle

The air-mass flow past the throttle \dot{m}_{th} is described well by the formula for flow through a restriction [3] [4]:

$$\dot{m}_{th} = \frac{C_d A_{th} p_{boost}}{\sqrt{RT}} \Psi\left(\frac{p_{man}}{p_{boost}}\right)$$

where A_{th} is the throttle plate open area, C_d the discharge coefficient, and $\Psi\left(\frac{p_{man}}{p_{boost}}\right)$ is

$$\Psi\left(\frac{p_{man}}{p_{boost}}\right) = \begin{cases} \sqrt{\frac{2\kappa}{\kappa-1} \left\{ \left(\frac{p_{man}}{p_{boost}}\right)^{\frac{2}{\kappa}} - \left(\frac{p_{man}}{p_{boost}}\right)^{\frac{\kappa+1}{\kappa}} \right\}} & \text{if } \left(\frac{p_{man}}{p_{boost}}\right) \geq \left(\frac{2}{\kappa+1}\right)^{\frac{\kappa}{\kappa-1}} \\ \sqrt{\kappa \left(\frac{2}{\kappa+1}\right)^{\frac{\kappa+1}{\kappa-1}}} & \text{otherwise} \end{cases}$$

By defining the coefficient K_{th} as

$$K_{th} = \frac{C_d A_{th}}{\sqrt{R}} \quad (1)$$

and

$$\beta(T, p_{boost}, p_{man}) = \frac{p_{boost}}{\sqrt{T}} \Psi\left(\frac{p_{man}}{p_{boost}}\right)$$

the flow \dot{m}_{th} can be rewritten as

$$\dot{m}_{th} = K_{th} \beta(T, p_{boost}, p_{man}) \quad (2)$$

From \dot{m}_s , T , p_{boost} , and p_{man} -data collected during the test cycle, the K_{th} coefficient can for each sample be computed as

$$K_{th} = \frac{\dot{m}_s}{\beta(T, p_{boost}, p_{man})}$$

if dynamics is neglected and therefore $\dot{m}_{th} = \dot{m}_s$. This calculated K_{th} coefficient is plotted against throttle angle in Figure 3. It is obvious that the throttle angle by its own describes the K_{th} coefficient well. From Equation 1, we see that the K_{th} coefficient is dependant on the throttle plate open area A_{th} . A physical model of this area is

$$A_{th} = A_1(1 - \cos(a_0\alpha + a_1)) + A_0$$

where A_1 is the area that is covered by the throttle plate when the throttle is closed and A_0 is the *leak area* present even though the throttle is closed. The parameters a_0 and a_1 are a compensation for that the actual measured throttle angle may be scaled and biased because of production tolerances. If values of $C_d A_0 / \sqrt{R}$, $C_d A_1 / \sqrt{R}$, a_0 , and a_1 are identified from the data shown in Figure 3, this results in a model of the K_{th} coefficient as function of the throttle angle α . In Figure 3, this model is plotted as a dashed line and we can see that the match to measured data is almost perfect except for some outliers for low throttle angles. This means that it is possible to assume that the discharge coefficient C_d is constant and independent of throttle angle. In conclusion, the K_{th} coefficient together with Equation 2 defines the model of the air-mass flow past the throttle.

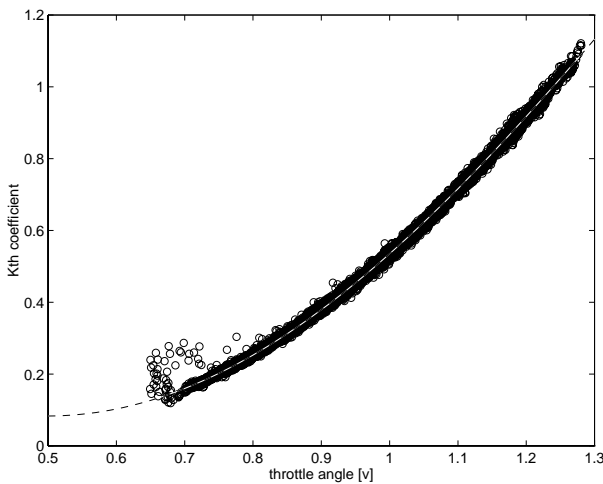


Fig. 3. The K_{th} coefficient for different throttle angles. It is obvious that the throttle angle by its own describes the K_{th} coefficient well.

3.2. Model of Air Flow into Cylinders

There are no accurate and simple physical models describing the flow from the manifold into the cylinders. Therefore a black box approach is chosen. From the mapping data, the air-mass flow is, in Figure 4, plotted against engine speed and manifold pressure. The preliminary model of the air flow into the cylinder \dot{m}_{cyl} consists of a linear interpolation of the data in Figure 4. It is assumed that the manifold temperature variation do not affect the flow substantially. In the indoor experimental setup used, with the engine operating approximately constant temperature, there was no way to validate this assumption.

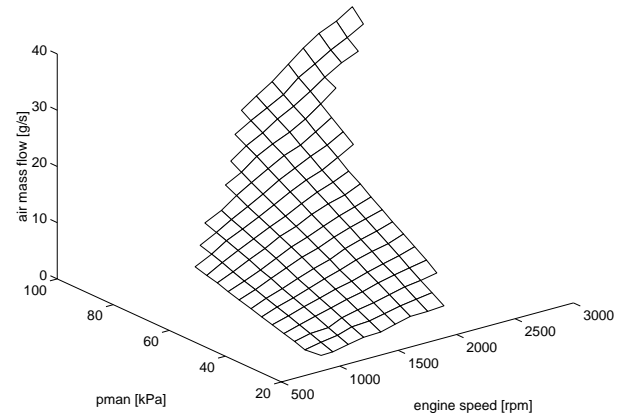


Fig. 4. The air flow out from the manifold into the cylinders as a function of engine speed and manifold pressure.

When the engine operating point, defined by engine speed and manifold pressure, leaves the range where mapping data is available, it is not possible to do interpolation. Because the mapping range is chosen to match normal operating, this happens rarely, but when it happens, the model will produce no output data.

For the construction of the final model, also data from the test cycle were used. To incorporate these data in the model, a parametric model including four fitting parameters are introduced:

$$\hat{m}_{cyl} = b_0 \text{interpolate}(n, p_{man}) + b_1 n + b_2 p_{man} + b_3 \quad (3)$$

The parameters b_i were found by using the Least-Square method. The benefit with this approach, i.e. to use of interpolation in combination with a parametric model, is that it is possible to include both test-cycle data and nonlinear mapping data when building the model. In addition, the parametric model provides for a straightforward way to adapt the model for process variations and individual-to-individual variations. Also the throttle model, described in the previous section, with its four parameters, has this feature.

3.3. Model Validation

The models (2) of \dot{m}_{th} and (3) of \dot{m}_{cyl} are validated during the FTP-75 test-cycle. Data were chosen from another test run, so the modeling data and the validation data were not the same. The upper plot of Figure 5 shows the measured air flow \dot{m}_s and the estimated air flow, for the two models respectively. Only one curve is seen, which means that the estimated air flow closely follows the measured. In the middle and lower plot, the difference between measured and estimated air flow are shown for both models respectively. It is again seen that both models manage to estimate the measured air flow well.

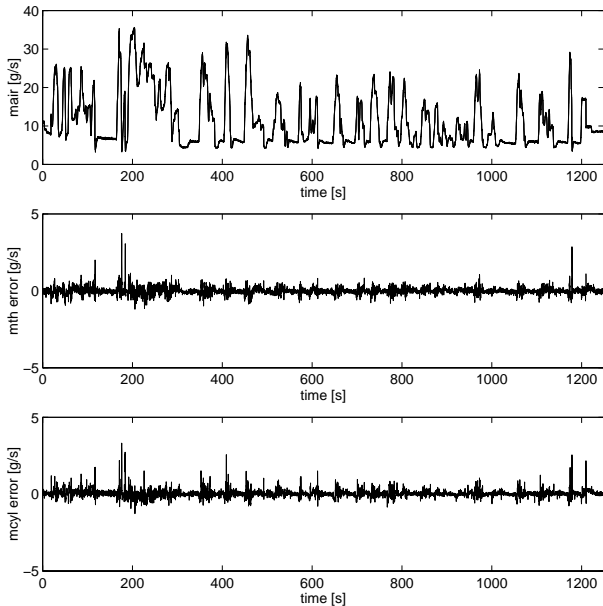


Fig. 5. The upper plot shows measured and estimated air-mass flow. The other plots show the model error for \dot{m}_{th} and \dot{m}_{cyl} respectively.

4. AIR LEAKAGE MODEL

When a leak occurs, air will flow out of or into the air-intake system depending on the air pressure compared to ambient pressure. By using the measured air flow \dot{m}_s , and the values $\hat{\dot{m}}_{th}$ and $\hat{\dot{m}}_{cyl}$ from the models (2) and (3) respectively, leakage air-flow can be estimated as

$$\Delta\dot{m}_{boost} = \dot{m}_s - \hat{\dot{m}}_{th}$$

for boost leakage and

$$\Delta\dot{m}_{man} = \hat{\dot{m}}_{th} - \hat{\dot{m}}_{cyl}$$

for manifold leakage.

Figure 6 shows $\Delta\dot{m}_{boost}$ and $\Delta\dot{m}_{man}$ for a case where a 6.5 mm boost leak is present. In the lower plot it

can be seen that $\Delta\dot{m}_{man}$ is almost zero, meaning that no leak air is added or lost in the manifold. However in the upper plot it is seen that measured air flow deviates from the estimate $\hat{\dot{m}}_{th}$, which means that air is lost somewhere between the air-mass flow sensor and the throttle.

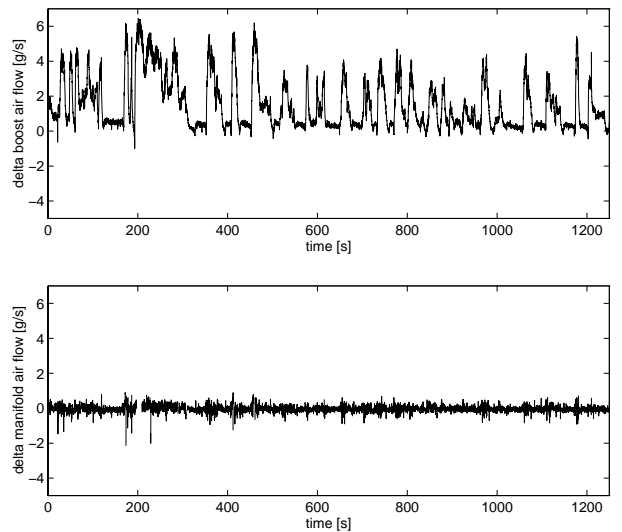


Fig. 6. The upper plot shows $\Delta\dot{m}_{boost}$ and the lower plot $\Delta\dot{m}_{man}$ when a 6.5 mm boost leak is present.

Thus by looking at the level and also the variance of $\Delta\dot{m}_{boost}$ and $\Delta\dot{m}_{man}$, it is possible to roughly detect when a leak is present. However to accurately estimate the size of the leak becomes difficult. To obtain high performance in terms of detecting leaks accurately a more sophisticated approach is needed; we need to model the air flow through the leaks.

4.1. Model of Boost Leaks

In the engine used in this work, the boost pressure is during normal operation always higher than ambient pressure. This means that the air flow through a boost leak will always be in the direction out from the air tube. One possibility is to model this air flow as an air flow through a restriction, like the model for flow past the throttle. If the equations used for the throttle model are reused, we arrive at

$$\dot{m}_{boostLeak} = K_{boost}\beta(T, p_{boost}, p_{amb}) \quad (4)$$

where the coefficient K_{th} has been replaced by K_{boost} , which now includes the area of the *leak*. This equation has only one unknown which is K_{boost} . The ambient pressure p_{amb} is not unknown because the engine is also equipped with a pressure sensor for measuring ambient pressure.

4.2. Model of Manifold Leaks

During most part of the operation of the engine, the manifold pressure is below ambient pressure. Therefore a manifold leak will mostly result in an air flow in the direction into the manifold. This flow is modeled in the same way as the model of flow through boost leaks, that is

$$\dot{m}_{manLeak} = K_{man}\beta(T, p_{amb}, p_{man}) \quad (5)$$

In the case the manifold pressure is higher than ambient pressure, which can occur because of the turbo-charger, the leak air-flow will be in the opposite direction and with p_{amb} and p_{man} in (5) changing places.

4.3. Validation of Leak Flow Models

For the validation of these leak models, different leaks were applied to the engine and the FTP-75 test-cycle was used. First “well behaved” leaks with known area, according to Section 2, were applied. The leaks ranged from 1 to 8 mm in diameter.

In Figure 7, a boost leak with 5 mm diameter, i.e. 19.6 mm², has been applied and data collected during a test cycle has been used to calculate $\Delta\dot{m}_{boost}$ and $\Delta\dot{m}_{man}$. In the upper plot, estimated air flow through the boost leak $\Delta\dot{m}_{boost}$ is plotted against p_{boost} . In the lower plot, estimated air flow through the manifold leak $\Delta\dot{m}_{man}$ is plotted against p_{man} . It is seen in the upper plot that for boost pressures close to ambient pressure (100 kPa), the estimated air flow through the leak is around zero. For higher boost pressures, the leak air-flow increases. The estimated air flow through the manifold leak is around zero for all manifold pressures.

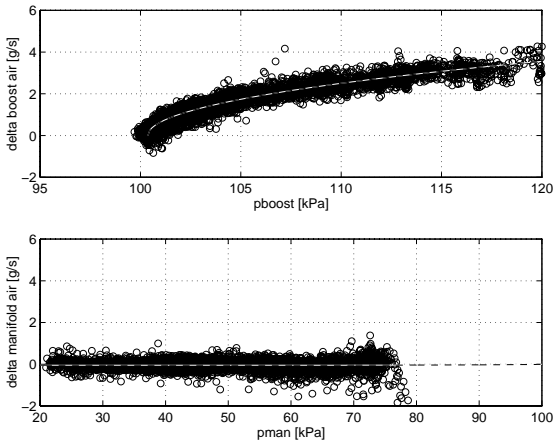


Fig. 7. Estimated air flow through boost leak (upper plot) and manifold leak (lower plot) when a 5 mm (diameter) boost leak is present.

Correspondingly for a manifold leak with 5 mm diameter, i.e. 19.6 mm², Figure 8 shows similar data. This

time it is the estimated flow through the boost leak that is around zero and the estimated flow through the manifold that differs from zero. For the data collected in the test cycle, the manifold pressure is always less than ambient pressure. This results in a $\Delta\dot{m}_{man}$ which is always positive.

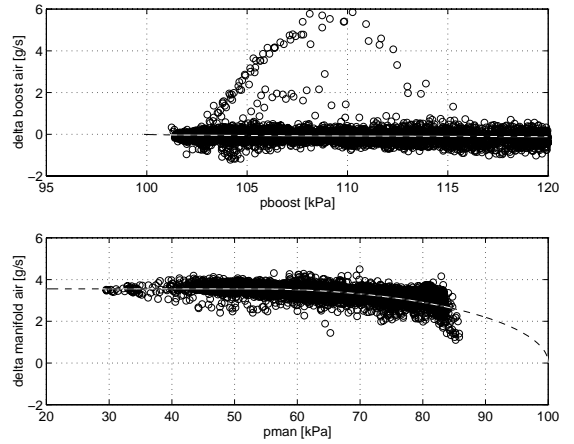


Fig. 8. Estimated air flow through boost leak (upper plot) and manifold leak (lower plot) when a 5 mm (diameter) manifold leak is present.

From Figures 7 and 8, it can be concluded that it is, from the estimations $\Delta\dot{m}_{boost}$ and $\Delta\dot{m}_{man}$, possible to conclude if there is a leak and if the leak is before or after the throttle. Also included in Figures 7 and 8 are the outputs from the models (4) and (5) of the leak air-flow. These are represented by the dashed lines. For each case, the coefficients K_{boost} and K_{man} have been obtained by using the Least-Square method to fit the curves to the data in the plots. Except for some outliers, which are very few compared to the total amount of data, it is seen that the estimated leak air-flows are described well by the models (4) and (5).

To validate this principle in the case of more realistic leaks, an experiment were performed in which the tube between the intercooler and the throttle was loosened at the throttle side. This had the effect that air leaked out from the system just before the throttle. In Figure 9 the estimated leak air-flows are again plotted against boost and manifold pressure respectively. It can be seen that also for this “realistic” leak, the model (4) is able to describe the leak air-flow well.

5. ESTIMATION OF LEAKAGE AREA

The coefficients K_{boost} and K_{man} are, according to the leak flow models, proportional to the leakage area. This is validated in the following experiment. The K_{boost} and K_{man} coefficients were obtained by fitting the leak flow models to measurement data, for leakages with six different diameters: 1, 2, 3.5, 5, 6.5, and 8 mm. For the

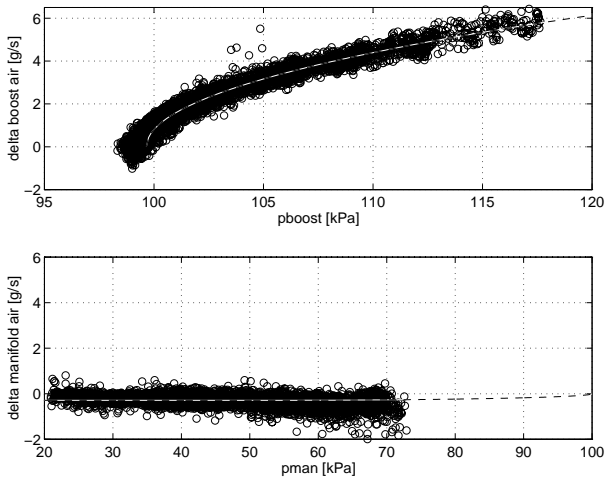


Fig. 9. Estimated air flow through boost leak (upper plot) and manifold leak (lower plot) when a realistic boost leak is present.

manifold leak it was only possible to use the first five diameters, because the air-fuel mixture became too lean for the 8 mm hole.

The result of this study is shown in Figure 10 in which the estimated K_{boost} and K_{man} coefficients are plotted against leakage area. The estimated K_{boost} coefficient is plotted as solid lines and the estimated K_{man} coefficient for manifold leaks is plotted as dashed lines. Both boost leaks and manifold leaks were studied. The experiments with boost leaks are marked with circles and the experiments with manifold leaks are marked with x-marks. It is seen in the figure that the K_{boost} and K_{man} coefficient are close to linearly dependant on the leakage area. Also seen is that the coefficient that should be zero for each leak case, is close to zero for both boost and manifold leakages. The estimations of K_{boost} for the case when a boost leak is present, and K_{man} for the case when a manifold leak is present, differs by a factor. One explanation is that because the bolts in these two cases, were mounted differently, the discharge coefficient were different even though the leakage area were equal.

From the Figure 10 it can be concluded that it should be no problem to detect the hole with 2 mm diameter corresponding to an area of 3.1 mm². However for the hole with 1 mm diameter corresponding to an area of 0.8 mm², the estimated K_{boost} and K_{man} coefficients are very close to zero. This means that in the presence of model uncertainties and measurement noise, the 1 mm hole is impossible to distinguish from the case with no leakage.

In conclusion, the described method is a way to, from measured data from the engine, estimate an *equivalent* area of possible leaks. Then if this estimated area, i.e. the K_{boost} and K_{man} coefficients respectively, becomes higher than a threshold, an alarm should be generated.

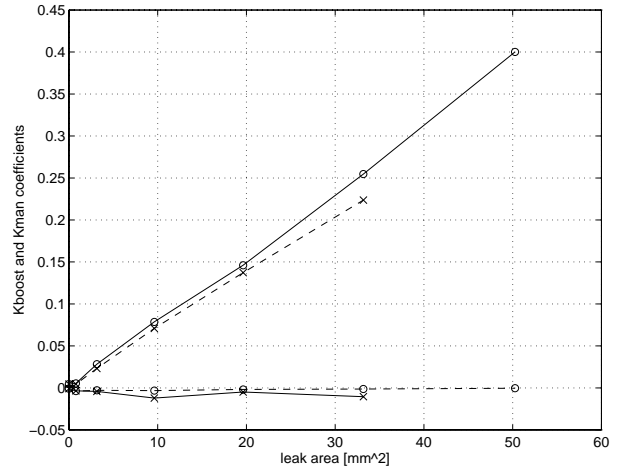


Fig. 10. Estimated K_{boost} coefficient (solid) and K_{man} coefficient (dashed), vs leak area when boost leak is present (circles) and when manifold leak is present (x-marks).

For the “realistic” leak which is illustrated by Figure 9, the K_{boost} coefficient is estimated to a value $K_{boost} = 0.26$. This corresponds to an equivalent area of 34 mm².

6. ON-LINE IMPLEMENTATION

For use in a real vehicle, an on-line implementation of the techniques described in the previous section is desirable. One simple approach, that is also computationally efficient, is to use the RLS algorithm [5]. In the case of estimating K_{boost} , the criterion

$$\sum_{k=0}^t \lambda^{t-k} (\Delta \dot{m}_{boost}(k) - K_{boost} \beta(T(k), p_{boost}(k), p_{amb}(k)))^2$$

is to be minimized at each time step t , and thus the estimation is obtained as a function of time. Depending on the choice of λ , convergence time is traded against accuracy.

This approach is demonstrated in Figures 11 and 12. Also for this experiment, the FTP-75 test-cycle was used. After approximately 500 seconds, a leak was applied. The upper plot in both figures shows the K_{boost} estimate and the lower plot the K_{man} estimate. It is seen that the K_{boost} estimate in both figures have discontinuities. The reason is that the on-line estimation of K_{man} is applied only when the boost pressure is higher than 102 kPa. This is because for boost pressures close to ambient pressure, the air flow through the boost leak is very small which means that the measurement data will contain no or very little information about the value of the K_{boost} coefficient. If also these data were used, the K_{boost} estimate would easily drift away from its real value.

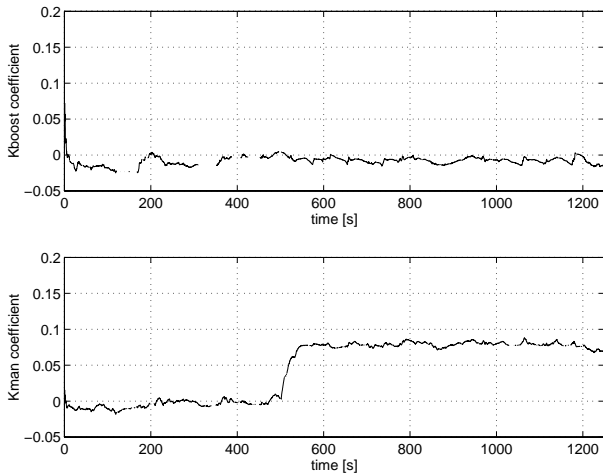


Fig. 11. On-line estimation of the K_{boost} coefficient (upper plot) and K_{man} coefficient (lower plot) when a 3.5 mm (diameter) manifold leak occurs at around $t = 500$ s.

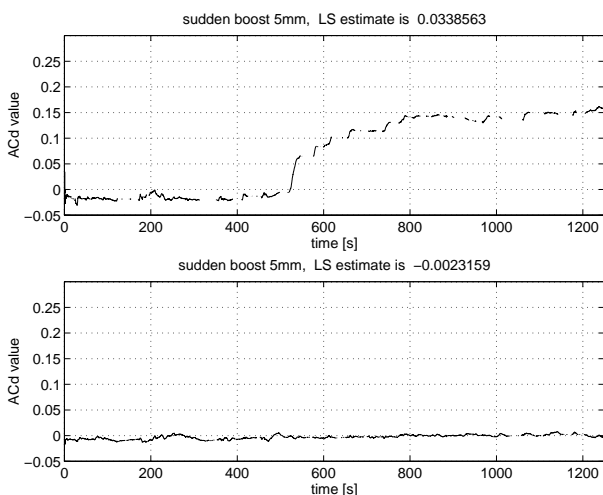


Fig. 12. On-line estimation of the K_{boost} coefficient (upper plot) and K_{man} coefficient (lower plot) when a 5 mm (diameter) boost leak occurs at around $t = 500$ s.

In Figure 11, the leak is a 3.5 mm manifold leak and it can be seen that the K_{man} estimate responds quickly when the leak occurs. Similarly in Figure 12, we see how the K_{boost} estimate responds when a 5 mm boost leak occurs. In this case the estimate converges more slowly. The reason is, as said above, that the estimation is only active when the boost pressure is higher than 102 kPa.

7. CONCLUSIONS

This work has presented a method for accurately detecting and diagnosing leaks in the air-intake system of an

SI-engine. The results are developed for a turbo-charged engine but they are also valid for a naturally aspirated SI-engine.

The method includes a physical model of the leaks. The diagnosis then becomes a parameter identification problem. Included in the method is an estimation of leakage area. By knowing the area, the engine management system can easily determine when to generate an alarm. Also it is possible to reconfigure the control algorithm in such a way that, the effect of the leak on emissions, is suppressed.

As small leaks as 2 mm in diameter, i.e. 3.1 mm^2 , can be detected. It is also possible to distinguish between leakages before or after the throttle. Because the method can be formulated as an RLS-algorithm, it is suitable for on-line implementation.

8. ACKNOWLEDGMENTS

This research is supported by NUTEK (Swedish National Board for Industrial and Technical Development) and SAAB Automobile AB.

REFERENCES

- [1] California's OBD-II regulation (section 1968.1, title 13, california code of regulations), resolution 93-40, july 9. pages 220.7 – 220.12(h), 1993.
- [2] E. Hendricks. Mean value modelling of spark ignition engines. *SAE-Technical Paper Series*, (900616), 1990.
- [3] John B. Heywood. *Internal Combustion Engine Fundamentals*. McGraw-Hill series in mechanical engineering. McGraw-Hill, 1992.
- [4] Charles Fayette Taylor. *The Internal Combustion Engine in Theory and Practice*. The M.I.T. Press, second edition, 1994.
- [5] Lennart Ljung. *System Identification: Theory for the User*. Prentice Hall, 1987.